Development of Micro-Debond Methods for Thermoplastics Including Applications to Liquid Crystalline Polymers

B. B. Sauer[a]; N. V. Dipaolo[a]

[a] DuPont Central Research and Development, Wilmington, DE, USA

PLEASE SCROLL DOWN FOR ARTICLE

Development of Micro-Debond Methods for Thermoplastics Including Applications to Liquid Crystalline Polymers

B. B. SAUER and N. V. DIPAOLO

DuPont Central Research and Development, Wilmington, DE 19880-0356, USA

Micro-bead and related debond techniques were used to study adhesion of liquid crystalline copolyesters (LCPs) and other semi-crystalline thermoplastic polymers to glass fibers. For polymers with poor flow even at high temperatures, symmetric beads on fibers were difficult to prepare so an alternative sample preparation method was developed where glass fibers were inserted into thin sections of molten polymer. Glass fibers of widely-varying diameters were used in order to extend the dynamic range of the debond techniques in terms of debonding area, showing a significant improvement in precision over that demonstrated previously with micro debond techniques. The fibers were freshly prepared in our laboratory and silane coated when necessary, which allowed us to minimize fiber surface heterogeneity effects which are believed to influence strongly debond test results. It was found that chemical bonding of the LCPs was quite favorable as was indicated by fracture surface analysis and by comparison with the shear strength of the neat resins. The apparent poor interphase strength in fiber-reinforced LCP composites is proposed to be due to orientation of the LCP molecules near the fiber interface leading to a cohesively weak layer of LCP near the interface. Reactive silane coupling agents lead to no improvement in interface strength as compared with bare glass because chemical reaction occurs on both surfaces. This results in very strong interfaces leading to polymer cohesive failure near the interface of all thermoplastics studied here

INTRODUCTION

One of the most direct methods for interface strength determination is the single fiber pull-out technique.[1-4] Alternatives include mechanical tests of composites, but the results are generally complicated by test geometry and composite and fiber morphology. The disadvantage of the single fiber pull-out tests is that the results are not necessarily well correlated with actual composite "interphase" properties. In many cases, the effective composite interphase properties are dominated by fiber-fiber interactions and other related morphological effects that one cannot address with single fiber pull-out or related tests. Other tests such as micro-compression[5,6] can be applied to real composites as an alternative to standard mechanical tests.

Related single fiber methods such as critical length, micro-compression, and micro-bead debond techniques have been compared with the single fiber pull-out re-

sults.[4, 7−9] with some degree of agreement depending on the polymer/fiber combination. The micro-bead debond (MBD) or pull-out technique[10] is a more recent modification of the single fiber pull-out technique and it is shown that there are some advantages in sample preparation of small contact area beads on small diameter fibers. Small contact areas lower the friction contribution in addition to minimizing fiber tensile failure during attempted debond tests. The majority of the MBD literature concerns epoxies and polyesters which can be cured after preparation of the liquid micro-bead.[10−12] Data for high temperature thermoplastics are scarce due to difficulties in sample preparation, although results for some thermoplastics such as poly(butylene terephthalate),[13, 14] poly(phenylene sulfide),[14] poly(ether ketones)[14, 15] are available mainly for Kevlar® and carbon fibers.

To overcome some of the experimental difficulties that we encountered with the bead micro-debond method, we have developed a "micro-film" debond technique which is somewhat similar to the fiber pull-out technique,[2] except that a micro-vise is used when fracturing the interface. For the few systems that we have studied where comparisons can be made, we have found that the micro-film and micro-bead techniques give identical results. The single fiber micro-film debond technique was found to be more versatile for high temperature thermoplastics such as LCPs with poor melt flow characteristics.

Several reports using MBD[10−12] and fiber pull-out[4, 16] methods have commented on the possible effect of roughness or surface chemical heterogeneity in terms of scatter in the debond force $vs.$ contact area plots which are related to interface strength. Certainly, Kevlar® and carbon fiber surfaces are not smooth or homogeneous, so in cases of adhesive failure, this can be very important in governing debond properties.[11] It has also been suggested that less than perfect droplet preparation leads to scatter in many cases. For the standard application of epoxy droplets, one must be careful not to allow thin skins of polymer to extend past the main bead boundaries, otherwise apparently larger pull-out forces are measured.[17] Inaccurate determination of fiber diameters is also a probable source of scatter.[12]

Some controversy exists in the literature regarding as to whether brittle failure occurs suggesting that debonding should be described by an energy criterion[4, 7, 8, 16, 18, 19] or whether the interface fails by shear yielding allowing one to assign an effective interphase shear strength.[4, 18] A signature of brittle fracture in a typical MBD or single fiber pull-out experiment, where only the embedded length (l) is varied, is a dependence[4, 18] of debonding force (F) on $l^{1/2}$ as opposed to the typical linear dependence of F on l for shear yielding systems.[4, 18] For failure by brittle fracture the energy criterion should be applied. At low l, Piggott[18] has shown that F for $both$ brittle fracture and shear yielding will vary linearly with l, which is relevant to our experiments where l is kept relatively small because of the low tensile strength of glass. Even though F varies with $l^{1/2}$ for brittle fracture, it is predicted to vary linearly with diameter (d) for both brittle fracture and shear yielding[18] making it even more difficult to distinguish between the two failure mechanisms in our experiments where we vary the diameter of the glass fibers.

In cases of brittle fracture, where fracture resistance is governing debonding, additional scatter should be observed in the debond force $vs.$ embedded length plots.[15, 18] Data presented later in this paper are consistent with this for the only

"brittle" system that we have studied. Because of the high scatter, in cases of brittle fracture of "tough" materials such as epoxies the apparent interface shear strengths on certain specimens measured by pull-out or MBD tests can sometimes be significantly larger than the bulk resin shear strengths,[20] because the resistance to fracture (*i.e.*, energy criteria) may be governing debonding forces.[4, 7, 8] Generally, for properly prepared specimens, the interphase shear strength should be less than or equal to the shear strength of the bulk resin when measured by the MBD method for shear yielding systems.

A large volume of information exists on interfacial chemistry and subsequent adhesion of polymer melts to solids. Isotropic polymer melts such as nylon 66 or poly(ethylene terephthalate) (PET) are well known to react at solid surfaces leading to strong interfacial bonds,[21, 22] and good reinforcement by fibers (Table I). At typical molecular weights, these semi-crystalline polymers are tough and would be expected to fail by shear yielding.[8] "Dry" adhesion is good for matrices like polyesters on both bare and reactive-silane-coated surfaces.[21, 22] The main contribution of reactive silanes (*e.g.*, aminopropylsilane, APS) is reduced environmental attack of the interphase.[22] More specifically, the glass surface is protected by silanes from attack by water, because the relatively hydrophobic nature of the APS layer reduces capillary penetration.[21, 22] Little is known about the chemical reaction of liquid crystalline polymer melts with solid surfaces although the interfaces are believed to be weak because very little reinforcement by fibers is observed, as can be seen by the minimal improvement in tensile properties in LCPs composites as compared with PET (Table I). The observance of apparently "bare" fibers in LCP-composite fracture surfaces is also another indication that the interphase strengths are low, although the results presented below show that the actual interface strength is relatively high, and that these fiber surfaces are not really bare.

Molten PET and nylon 66 are known to be chemically reactive with solid surfaces at the molding temperatures.[22] Likely reactions of PET chain ends with amine groups associated with an APS coating are indicated in the schematic in Figure 1A. Chain scission leading to grafting of PET chain segments onto the APS coated surfaces are also possible (Fig. 1B). Similar reactions of both chain ends and main chain ester groups with the surface hydroxyl groups on bare glass surfaces are also favorable. Both of these will lead to chemical bonding of the polymer matrix with the fiber, leading to good adhesion and good reinforcement of PET (Table I) with glass fiber. The same end

TABLE I

Tensile Strengths of Neat Resins and their Short Dicontinuous Glass Fiber Reinforced Composites (in MPa)

	Neat Resin	30% Glass
LCPs		
HX 4000	83	95
Vectra® A950	165	180
Isotropic Polymer		
PET (M_w, *ca.* 40 kg/mol)	~ 86	160

(A)

$$\text{Glass} \sim \text{NH}_2 + \overset{\overset{\displaystyle O}{\|}}{\text{H-OC}} \text{- PET} \rightarrow \text{Glass} \sim \overset{\overset{\displaystyle O}{\|}}{\text{N-C}} \text{- PET} + \text{H}_2\text{O}$$
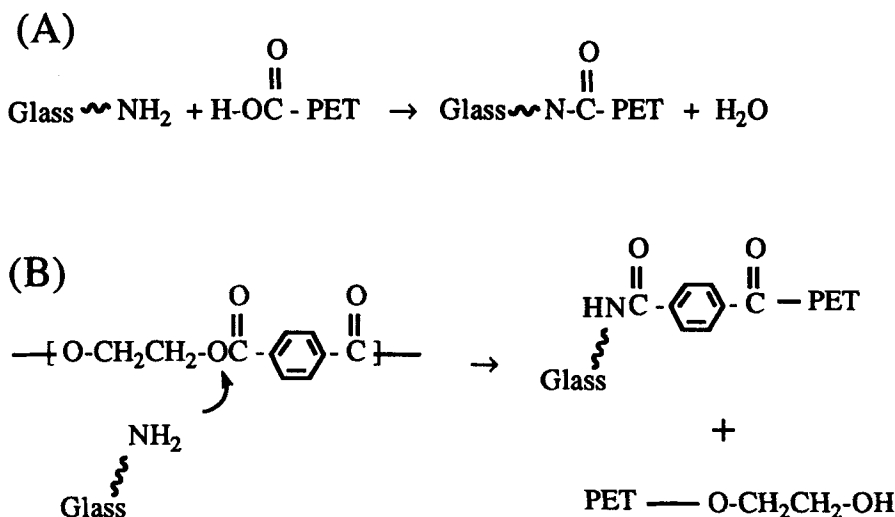
(B)

FIGURE 1   (A) Schematic of amine functionality on glass due to APS coating and its possible reaction with the acid end-groups on PET leading to chemically bound chains. (B) Chain scission of PET by amine functionality on glass leading to chemical grafting of PET to APS-treated glass.

groups are present on the copolyester LCPs studied here. Also, the main chain ester groups in the LCPs should be susceptible to the same chain scission and subsequent chemical grafting to fiber surfaces as in the case of isotropic polyesters such as PET. As will be seen below, this is indeed the case and one must consider the strong chemical bonding of LCPs to the surface when attempting to understand its adhesion properties.

EXPERIMENTAL

Materials

Poly(ethylene terephthalate) (PET) and nylon 66 (Zytel® 101) were dried at 100°C for 24 hrs. PET samples were used with weight average molecular weights (M_w) on the order of 40 k. At this MW PET is strong and relatively tough and can be easily molded or spun into fibers. PET with $M_w = 10$ k was obtained by hydrolysis of 40 k PET for 5 minutes at 300°C. Vectra® A950 is a semi-crystalline random copolyester of hydroxy benzoic acid (HBA, 0.73 mole fraction) and hydroxy naphtholic acid (0.27). Vectra® has a glass transition (T_g) of ca. 100°C and $T_m = 300$°C. HX4000 is one of DuPont's wholly aromatic semi-crystalline random copolyesters with a T_m of 310°C and the composition given previously.[23] "LCPI" was a gift of R. Blume of DuPont and is a non-crystalline copolyester containing HBA, terephthalic acid, and 2, 3' dihydroxy 2' chlorobenzophenone with a T_g of 95°C.

E-glass fibers were made by drawing molten glass by hand after melting the glass in an oxygen/methane torch. γ-aminopropyl triethoxysilane (APS) was applied from a

2% solution in 5% water/95% ethanol mixture to give a *ca.* 100 Å thick "uniform" coating on the glass fibers.

Methods

To overcome some of the experimental difficulties with the MBD method, a so-called "micro-film" debond method was developed. As in the MBD method, the interface is fractured using the micro-vise. We found that the sample preparation method associated with the micro-film method (described below) is necessary because the micro-bead technique fails for high viscosity/high temperature systems such as Vectra® due to the formation of asymmetric beads due to poor flow, even after extensive annealing under a variety of conditions including inert atmospheres. The asymmetric beads cause the fibers to break before debonding because the fiber bends where the bead contacts the micro-vise. The other main advantage of the micro-film method is that we found that it was easier to prepare specimens with smaller embedded lengths (*l*) with all of the polymers studied, especially with thicker fibers. Because of the relatively low strength and toughness of glass, sometimes it was necessary to have embedded lengths only two or three times larger than the fiber diameter, which is difficult to attain with the bead method.

We also found that the ease of sample preparation, combined with our ability to use a wide range of fiber diameters, readily allowed us to access a large variation in contact areas, thus, effectively improving the precision of the measurement by several times for most systems. The variation in fiber diameter is probably not possible with Kevlar® or carbon. For the systems that we are interested in, adhesion is extremely strong so it is not possible to vary the imbedded length, *l*, significantly at constant diameter, without breaking the glass fiber during attempted debonding. The theoretical limitations of *l*, which depend on the fiber tensile strength, have been discussed previously.[10]

The standard analysis of micro-debond data indicates that if the interphase yields at a certain stress (τ), then assuming constant shear stress at the interface gives:[10, 16, 18]

$$\tau = F/(\pi \, d \, l) = m \, g/A \tag{1}$$

where *F* is the debond force measured on the Instron, *d* is the fiber diameter, *l* is the bead length or immersion length, *m* is the debond mass, *g* is the gravitational constant, and *A* is the contact area. In the single fiber pull-out method, *l* is the embedded length.[16] Even if brittle failure occurs as opposed to shear yielding, for values of *l*/*d* less than ∼ 5 the interface strength is predicted to be described by a linear dependence of *F* on *l*. Most of our data are characterized by small *l*/*d* and most polymers are tough and seem to fail by shear yielding of the interphase, as will be discussed below. We never observe any of the non-linearity in the *F* *vs.* *l* plots seen by other authors.[4, 10, 16, 18] For many of the systems we are interested in adhesion is extremely strong so it is not possible to increase the *l*/*d* ratio significantly without glass fiber tensile failure. We do vary the fiber diameter, as was discussed above.

A schematic of the standard micro-bead sample geometry is shown in Figure 2 (left hand side). Sample preparation is quite easy for polymers which flow well. Generally a polymer filament is tied in a small knot or looped over a glass fiber.[14] After heating, the filament immediately flows and forms a symmetric bead around the fiber, even in the
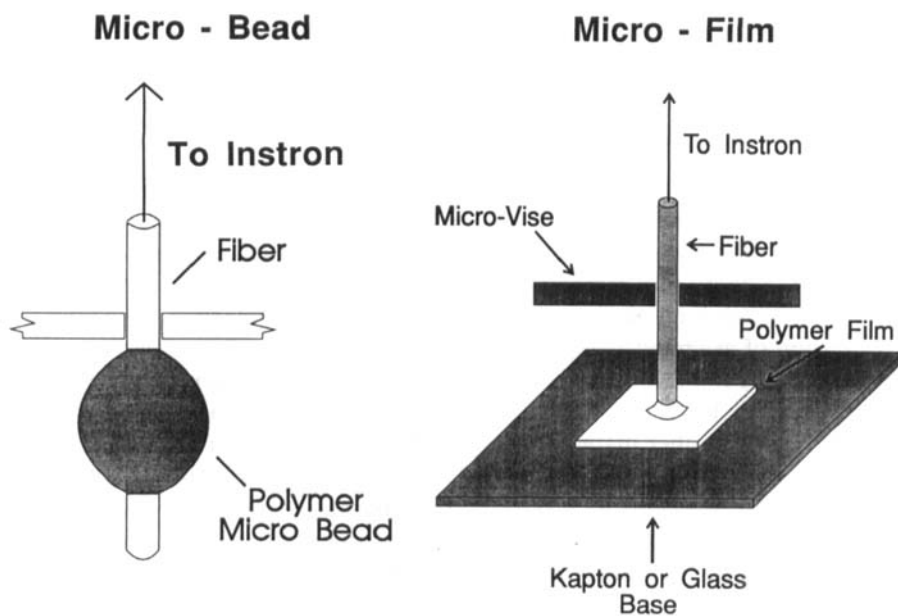
Micro - Bead

Micro - Film

FIGURE 2   Schematics of the sample geometries for the micro-bead debond and micro-film debond methods.

cases where the contact angle is zero,[24, 25] *i.e.*, in a complete wetting situation such as is known for PET on bare glass.[26] It has been shown that beads spontaneously form because the high radius of curvature of the fiber surface under these conditions.[25] Good samples using the bead method could only be prepared for PET, nylon 66, and LCP1. For Vectra® and HX4000, symmetric beads could not be formed due to poor flow of the polymer under these conditions. The fibers also broke the majority of the time for PET and nylon 66 because of the high debond mass relative to the fiber tensile strength. This was mainly due to our inability to make small beads reproducibly although some good data were obtained in the few cases where we did succeed in making small beads. The fiber micro-film debond method described below was generally more successful.

For the micro-film debond method the sample was prepared by placing a small piece of polymer film (area $\sim$ 5–20 mm^2) on a small square of a film of Kapton® ($T_m > 500°C$) or a glass coverslip (Fig. 2, right side). The film thickness should be a few times the fiber diameter. The film was placed on a hot plate at temperatures $\sim 10 - 100°C$ above the melting or softening point of the polymer and a glass fiber carefully pushed completely through the molten film. Then the sample was cooled and solidified keeping the fiber stationary. The pull-out force was measured in the normal way at 25°C using a microvise.[10] An actual specimen consisting of a thin PET film (400 μm thick) with a 106 μm diameter bare glass fiber inserted normal to the plane of the film is shown in Figure 3. The meniscus had crept up to the extent shown over a period of $\sim$ 30 seconds in the molten state at 280°C (the melting point of PET is 255°C). The rate is known to be strongly dependent on the fiber diameter with menisci on larger diameter fibers leading to much slower equilibration times.[26, 27] The shape of these menisci are not significant-
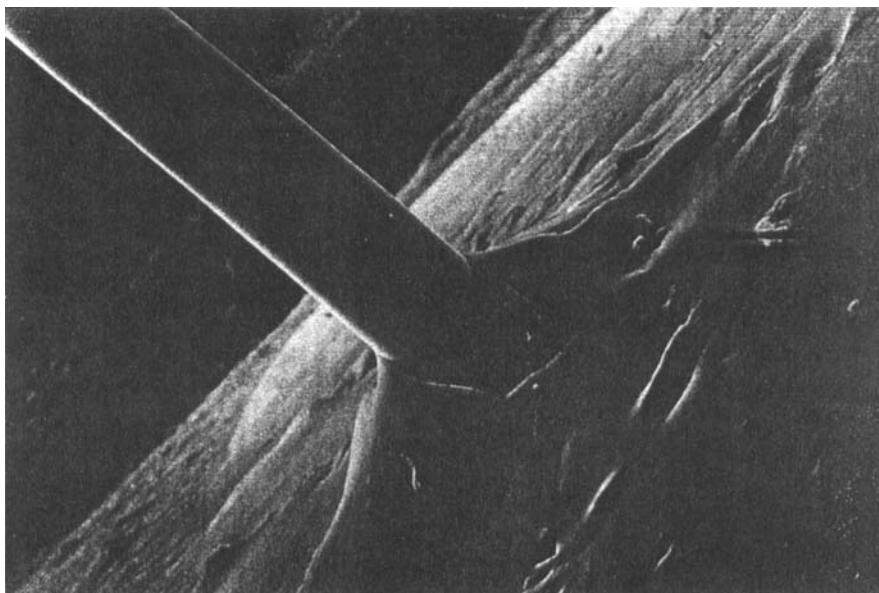
FIGURE 3   A SEM is shown for a sample prepared for the micro-film method. A 106 µm bare glass fiber is inserted normally into a thin film PET film (400 µm thick). The meniscus has crept up slightly over a period of ~ 30 seconds at 280°C.

ly different from the bead edges or bead "menisci". Micro-vise contact with the bead edges or film menisci typically leads to some damage in the strongly adhering cases (see discussion). With Vectra®, significant menisci do not form, at least on fibers with $d > 40$ µm, because the polymers do not flow well in the melt, even under inert atmospheres and/or at very high temperatures.

In most cases the contact area (A) was determined before and after fracture, if possible, by examining the debris on the glass fiber in the optical or electron microscope. One can also assess the degree of wetting for those polymers with poor melt flow, from viewing the fracture surfaces. For all polymers studied here, melt flow was sufficient to obtain intimate contact of the fiber immersed in a molten sheet of polymer, even if the meniscus does not creep up the fiber as it does with a polymer with good flow properties such as PET (Fig. 3).

RESULTS

Table II summarizes typical raw debond data for Vectra® indicating the typical fiber diameters and imbedded lengths used in our studies with variable diameter glass fibers. The Vectra® results will be discussed below. Most results for high MW PET on glass fiber were obtained using the micro-film debond method, because of problems with fiber tensile failure with samples prepared by the bead method. For PET or nylon 66,

TABLE II
Raw Micro-Film Debond Data for Vectra®: Bare and APS-Coated
Glass Fibers

	Speed mm/min	Mass kg	l μm	d μm	A mm^2	τ MPa
APS	0.1	0.59	500	170	0.267	21.7
APS	0.5	0.51	1000	60	0.188	26.0
APS	0.5	0.09	200	55	0.0345	25.5
Bare	0.25	0.325	500	90	0.142	22.4
Bare	0.25	0.301	650	80	0.163	18.1
Bare	0.25	0.16	250	90	0.071	22.1
Bare	0.5	0.30	550	80	0.138	21.3
Bare	0.5	0.117	300	60	0.057	20.1
Bare	0.1	0.207	500	60	0.094	21.6

values of l greater than $\sim 400\,\mu m$ usually led to fiber tensile failure instead of debonding. For experiments where the fibers did not break, we found that the film and bead debond methods gave the same results for PET of either MW. The lines in Figure 4 are weighted least squares fits and are forced through the origin. The slope is proportional to τ. The reactive silane coating (APS) had no effect on τ. Evaluation of
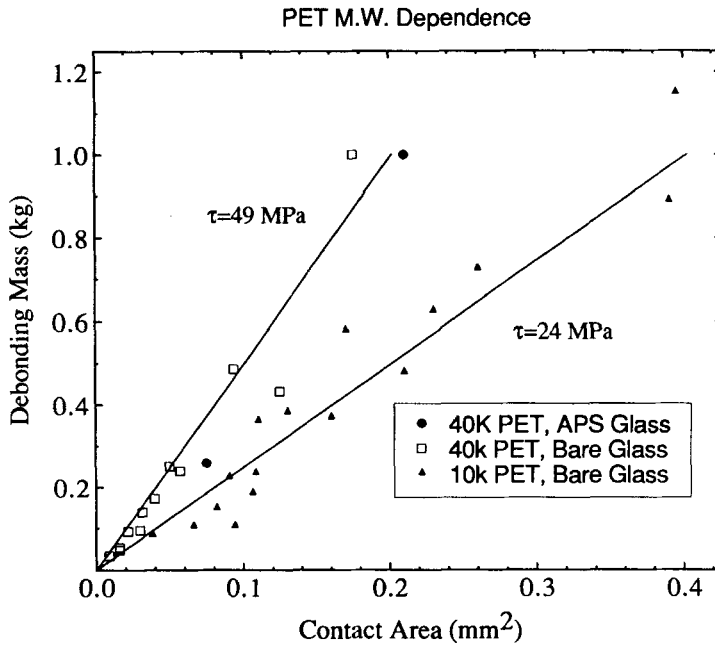

FIGURE 4   Debonding mass vs. contact area for PET of the different MWs indicated. Both bare and aminopropylsilane (APS) coated glass fibers were used.

the fracture surfaces indicated that cohesive failure of the PET near the interface occurred in most cases, rather than adhesive failure at the interface. Thus, the interface is stronger than the polymer near the interface. There is a factor of two difference in τ for the two molecular weights (Fig. 4 and Table I). Chemical reaction of PET leading to strong bonding at the interface should occur with both Mws.[22, 26] 10 k PET matrices are weak and brittle while 40 k PET is relatively strong and tough in the neat form. As expected, the matrix strength near the interface contributes to the large difference in τ between the two MWs. The data in Figure 4 also suggest that there is more scatter for the 10k PET. Although we have not completed detailed analysis of the fracture mechanisms, it has been suggested in the literature that if brittle fracture occurs, as compared with shear yielding, then more scatter in the debond data should be seen.[4, 15] The average interface shear strength of 24 MPa (Table III) is larger than the bulk shear strength estimated to be about 15 MPa for this low MW PET, suggesting that fracture resistance is important.[4, 7, 20] This is also consistent with a brittle fracture mechanism.

Data for LCP1 are shown in Figure 5. Of all the polymers, LCP1 was the easiest from which to prepare samples for both bead- and film-debond methods and the results show that there is no difference between the two. Since the scatter in the results is low, we found that only a few samples, i.e., a few data points, were needed to characterize the interphase shear strength in the samples. The limited data for the APS-coated fibers in Figure 5 suggest that the APS coating has no effect on the debond force, as was the case for all materials studied here. The interface strength of $\tau = 23 \pm 3$ MPa measured for LCP1 is significantly lower than that of PET and nylon 66.

The data for the other systems are shown in Figure 6, where the y-axis scales are all the same. The interface shear strengths are significantly lower for the two LCPs, HX 4000 and Vectra®, as compared with the isotropic polymers, PET and nylon 66 (Table

TABLE III

Interface Shear Strengths Determined Using Micro-Debond Methods Compared with Other Standard Tensile Properties

	τ^a, Interface Strength (MPa)	Tensile Strength, Neat Resin (MPa)	Shear Strength,[b] Neat Resin (MPa)
Isotropic Polymers			
PET ($M_w = ca.$ 40 kg/mol)	49 ± 5	86[c]	50[c]
PET ($M_w = ca.$ 10 kg/mol)	24 ± 7	26[d]	15[d]
Nylon 66	45 ± 3	70	41
LCPs			
Vectra® A950	23 ± 2	165 (25[e])	96 (15[e])
Vectra® A900	24 ± 2	–	–
HX4000	13 ± 2	83 (20[e])	48 (12[e])
LCP1	23 ± 3	–	–

[a] Errors are the approximate 95% confidence level.
[b] Shear strengths extimated using von Mises criteria, *e.g.*, 0.58 × Tensile Strength.
[c] Reference 30.
[d] Estimate is very qualitative because of difficulties in measuring tensile strengths of these brittle materials.
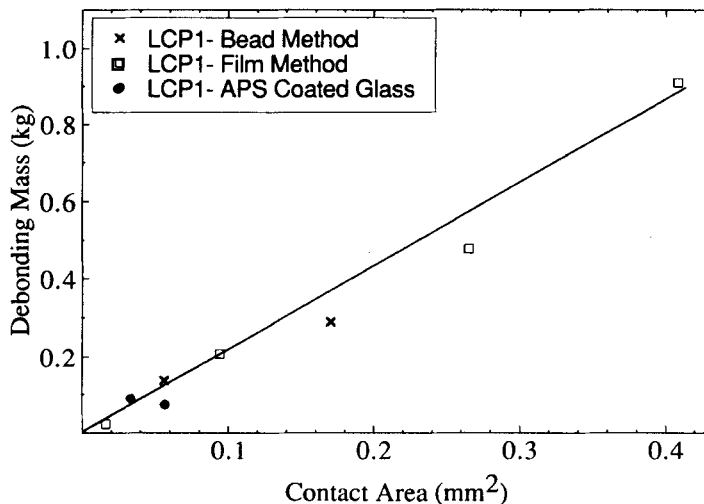[e] Transverse strengths.

FIGURE 5   Debonding mass vs. contact area for LCP1 of the different MWs indicated. Data were taken using the micro-film and micro-bead debonding methods. Both bare and aminopropylsilane (APS) coated glass fibers were used.

I). No significant difference in debond force was seen between the APS-coated fibers and bare glass. The raw data for Vectra® are listed in Table II to indicate typical dimensions in terms of the embedded lengths and diameters. The typical pull-out rates used in the literature are 0.5 to 1 mm/min.[7, 10, 28] Here we generally find no dependence of τ for rates ranging from 0.1 mm/min to 0.5 mm/min although higher rates give higher debond forces due to elastic energy storage and possibly a change in failure mechanism. At lower debond rates, the fracture surface of the glass fiber generally was found to have a thinner layer of LCP after cohesive failure. This is a general feature of fracture surfaces of composites which have failed at different rates.

The load vs. displacement curve obtained on the Instron® is shown in Figure 7 for debonding of a bead of LCP1. The data correspond to the specimen shown in Figure 8 (top) with a bead length of $l = 690$ μm on a 79 μm diameter glass fiber. The maximum mass at the debond point is 0.29 kg in Figure 7. After the maximum, effects of friction of the bead on the fiber are detected and are minimal in most cases. The electron micrograph in Figure 8 (top) corresponds to a bead which had been previously fractured. Some damage due to the micro-vise can be seen at the bottom of the bead. Figure 8 (bottom) shows the fiber fracture surface for this same sample. The original position of the bead is indicated by the horizontal arrows. There are regions of cohesively-failed LCP easily visible at this magnification. In cases where the SEM does not have sufficient resolution, single fiber wettability techniques, such as those applied by Penn and Lee,[16] indicate that the entire fracture surfaces for all of our LCP debonded samples are covered by at least a thin layer of LCP; i.e., no bare glass is detected in the fracture region.
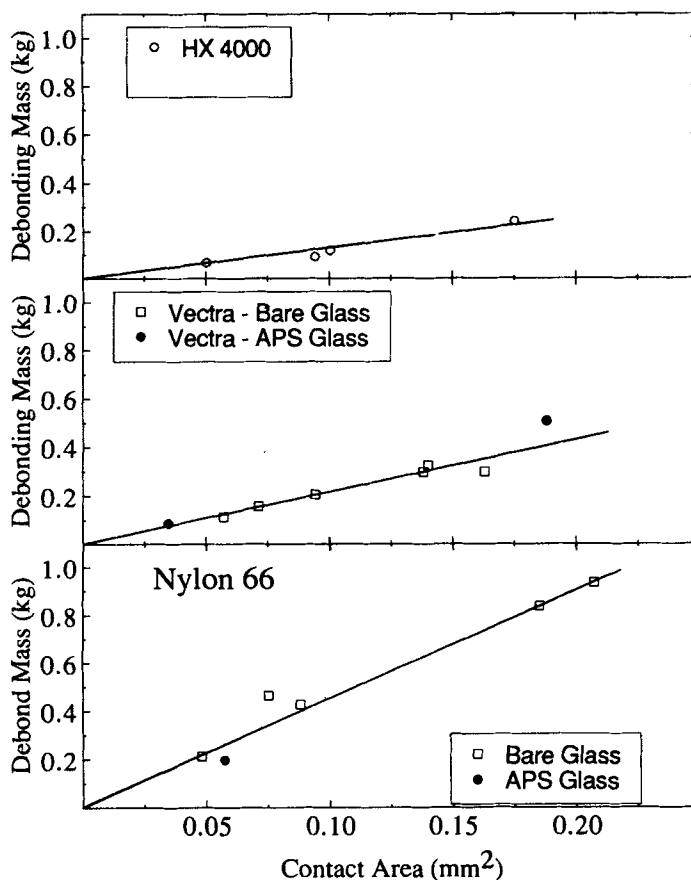
FIGURE 6   Debonding mass *vs.* contact area for the polymers indicated. Both bare and aminopropylsilane (APS) coated glass fibers were used.

DISCUSSION

Viewing the fracture surface in the optical and electron microscope gives some insight into the quality of sample preparation and also the mechanism of fracture. Generally, little polymer remains on the surface in the case of carbon fiber/epoxy,[2, 28] although a small ring of polymer is sometimes left over due to fracture of the bead meniscus. It has been shown in some systems, by wettability methods, that the carbon fiber/epoxy interface does not break, but instead the skin of the carbon fiber fails cohesively.[29] For LCPs, because of chemical bonding with the fiber surface, we always find that polymer cohesive failure occurs, leaving layers of LCP on the fiber varying in thickness from molecular (detected by wettability methods[16]) to macroscopic. The layers are generally relatively uniform in thickness for the LCPs and sometimes very thin and not visible by
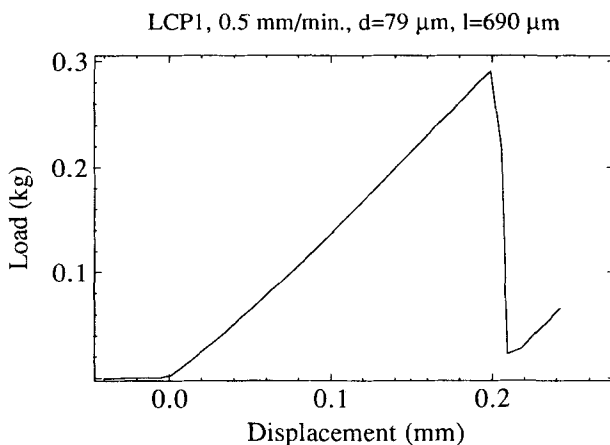
LCP1, 0.5 mm/min., d=79 μm, l=690 μm

FIGURE 7   The load *vs.* displacement curve measured on the Instron[R] is shown for a bead of LCP1 on an originally bare glass fiber.

SEM. For PET there is usually a thick ring of cohesively-failed polymer near the boundaries of the bead (or meniscus of the film), similar to that seen in other debond systems.[2,28] In a fraction of the samples, there is larger scale cohesive failure, leading to patches or layers of cohesively- failed PET, several microns thick, on the glass. For the lower molecular weight PET this is more often observed, presumably due to its low cohesive strength.

Further evidence that, in these "well bonded" systems, the debond techniques are really measuring the strength of the polymer near the interface, is found by comparing interphase properties (τ) with bulk tensile properties measured in a typical tensile strength test on test bars. Table III shows that τ for higher MW PET and nylon 66 are essentially the same as the bulk shear strengths of the neat resins, supporting the claim that it is the cohesive strength of the resin in the interphase region that is governing τ in these "well adhering" systems which fail by shear yielding. It is known that the strength of LCP moulded test bars are highly anisotropic as is indicated by typical longitudinal and transverse strength data in Table III. Taking the transverse (weak direction) tensile strengths for the LCPs where available, and converting them into transverse shear strengths using the von Mises criteria (*i.e.*, shear strength = 0.58 × tensile strength), one can see qualitative agreement between the bulk transverse shear strengths and τ. For example, in Vectra[R] $\tau = 23$ MPa, while the transverse shear strength is estimated to be 15 MPa. In HX 4000 the agreement between the two is closer (Table III). This is strong evidence that the origin of a cohesively weak interphase region, leading to the rather low values of τ compared with isotropic polymers, is a result of partial orientation of the LCP chains parallel with the fiber surface. This would lead to a cohesively-weak interphase region as is seen by the debond measurements. The low interphase shear strengths lead to poor reinforcement of LCP by fibers in discontinuous fiber composites (Table I), compared with better than 100% improvement in the tensile strength for a typical fiber-reinforced isotropic polymer.
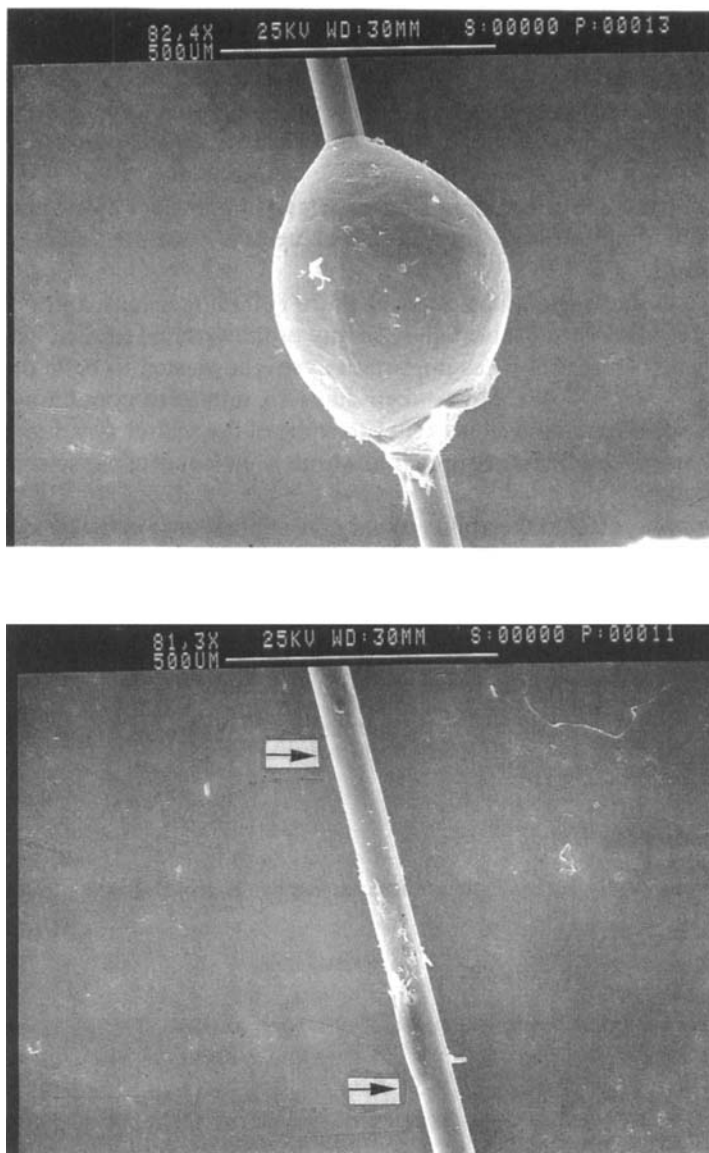
FIGURE 8 (Top) The specimen after fracture corresponding to the data in Figure 7 is shown. The fractured bead had $d = 79\,\mu$m and $l = 690\,\mu$m. (Bottom) The fracture surface is shown for same bead. The original position of the bead is indicated by the horizontal arrows. There are regions of cohesively-failed LCP easily visible at this magnification.

CONCLUSIONS

To conclude, we summarize some key factors in optimizing the quality of the data using the micro-debond techniques. The ideas are applicable to either micro-bead or micro-film debond methods:

1) Care must be taken to make sure that bead boundaries are sharp, *i.e.*, no smeared layers of film should extend past the main bead or film menisci.

2) Micro-vise edges should be adjusted very close to the fiber surface otherwise the values of τ will be artificially high because of compressive forces on the bead. Data obtained with non-adjustable vises could lead to inaccurate results because of this.

3) The fiber fracture surface should be examined in optical or electron microscopes after debonding to obtain an accurate value of l. Accurate values of d are also important.[12]

4) The fiber surfaces should be clean, chemically homogeneous, and smooth. Since we do not observe adhesive failure in any of the systems studied here, chemical heterogeneity may not be as important as it is suggested to be in other debond systems.[10, 11, 12, 16] We have taken steps to minimize contamination of the surfaces which probably contributes to some of the scatter in values obtained in the literature. Our fibers are prepared within a few hours of use so contamination is negligible.

5) We re-emphasize that the ability to vary the contact area in the debond methods, by varying the glass fiber diameters in addition to l, is very useful in extending the dynamic range of the determination of τ from the F *vs.* A plots. This contributes to the higher precision of the data compared with those reported in the literature, although the low scatter may also be partly due to a shear yielding rather than a brittle fracture mechanism in our systems. The use of tough and ductile thermoplastics, and not the experimental method, may in part govern the failure mechanism and thus the scatter in the debond results.

Acknowledgements

References

1. G. V. Shiriajeva and G. D. Andreevskaya, *Sov. Plastics* no. **4**, 40, (1962).
2. J. P. Favre and J. Perrin, *J. Mat. Sci.* **7**, 1113 (1972).
3. L. S. Penn and S. M. Lee, *Fib. Sci. Tech.* **17**, 91 (1982).
4. M. R. Piggott, D. Andison, *J. Reinforced Plastics and Comp.* **6**, 290 (1987).
5. J. F. Mandell, J. H. Chen and F. J. McGarry, *Int. J. Adhesion and Adhesives* **1**, 40 (1980).
6. E. J. H. Chen and J. G. Young, *Composites. Sci. Techn.* **42**, 89 (1991).
7. M. R. Piggott, *Polym. Eng. Sci.* **31**, 1246 (1991).
8. M. R. Piggott, in *Composite Applications: the Role of Matrix, Fiber, and Interface*, T. Vigo, B. Kinzing, Eds. (VCH Publishers, New York, 1992), p. 221.
9. C. Y. Yue and W. L. Cheung, *J. Mat. Sci.* **27**, 3843 (1992).
10. B. Miller, P. Muri and L. Rebenfeld, *Comp. Sci. Tech.* **28**, 17 (1987).
11. U. Gaur and B. Miller, *Compos. Sci. Techn.* **34**, 35 (1989).
12. B. Miller, U. Gaur and D. E. Hirt, *Compos. Sci. Techn.* **42**, 207 (1991).
13. K. P. McAlea and G. J. Besio, *SPE ANTEC Tech. Papers* **33**, 1458 (1987).
14. M. Gaur, G. Desio and B. Miller, *SPE ANTEC Tech. Papers* **35**, 1513 (1989).
15. S. L. Chuang, N.-J. Chu and W. T. Whang, *J. Appl. Polym. Sci.* **41**, 373 (1990).
16. L. S. Penn and S. M. Lee, *J. Comp. Tech. Res.* **11**, 23 (1989).
17. W. Uy, Personal Comm.
18. M. R. Piggott, *Comp. Sci. Tech.* **30**, 295 (1987).

19. R. J. Scheer, J. A. Nairn, *Compos. Eng.* **2,** 641 (1992).
20. M. J. Pitkethly and J. B. Doble, "*Proc. Int. Conf. on Interfaces in Composites,* F. R. Jones, Ed., Sheffield, UK, 1989, p. 35.
21. E. P. Plueddemann, *J. Paint Sci. Tech.* **42,** 607 (1970).
22. E. P. Plueddemann, *Silane Coupling Agents* (Plenum Press, New York, 1982).
23. R. E. S. Bretas, D. Collias and D. G. Baird, *Polym. Eng. Sci.* **34,** 1492 (1994).
24. F. W. Minor and A. M. Schwartz, *Textile Res. J.* **29,** 940 (1959).
25. B. J. Carroll, *J. Colloid Interface Sci.* **57,** 488 (1976).
26. B. B. Sauer, *J. Adhes. Sci. Techol.* **6,** 955 (1992).
27. B. B. Sauer and N. V. DiPaolo, *J. Colloid Interface Sci.* **144,** 527 (1991).
28. D. A. Biro, P. McLean and Y. Deslandes, *Polym. Eng. Sci.* **37,** 1250 (1991).
29. C. T. Chou, U. Gaur and B. Miller, *J. Adhesion* **40,** 245 (1993).
30. R. Ikeda, Personal comm.